

The flip-and-shift signal enhancement application for a predictive electron-beam pattern registration model

D. C. King, A. J. Steckl, J. L. Morgenstern, J. F. McDonald, M. A. Bourgeois, D. J. Yernc, and I. Elminkyawi

Center for Integrated Electronics, Rensselaer Polytechnic Institute, Troy, New York 12181

(Received 11 June 1985; accepted 9 October 1985)

A simple physical model based on an absorption-like mechanism has been developed for the backscattering of electrons from registration marks used in e-beam lithography pattern alignment. The model uses a signal with an exponential dependence on the traversed material path length. This model produces simulated registration signals in close agreement with experiments for marks with a variety of topological features. Error between data and simulation is less than 5%. The model has been used in investigations of novel registration signal manipulation schemes. Signal power resulting from the use of one such scheme, "flip-and-shift," is shown to be significantly greater than from simply summing individual detector signals.

I. INTRODUCTION

High density complex patterns for integrated circuits can be produced with great accuracy by e-beam lithography systems. One of the most critical steps in any lithography system is the spatial alignment of sequential layers.¹ The basic elements of this alignment process, known as pattern registration, are illustrated for e-beam lithography in Fig. 1.

The lithography tool used for experimentation in this work is the IBM EL-2 located at Rensselaer Polytechnic Institute in Troy, New York. In this machine, the wafer, which contains many chip sites, resides on an x - y stage at the bottom of the e-beam column. After the stage positions the desired site in the writing field, the electron beam scans over the expected location of fiducial marks on the wafer surface in a raster pattern perpendicular to the long edges of the marks. The incident electrons penetrate the wafer surface and collide with molecules, causing backscattering. Many of the backscattered electrons escape from the substrate surface and subsequently reach four detector diodes positioned above the wafer.

Each of the four detectors produces an output dependent upon the number and energy of received electrons. The output of each detector feeds a current-to-voltage converter. The resulting four voltage signals constitute the components of the total registration signal.

By observation, it is known that the signal from a given detector is a function of the detector position relative to the fiducial mark and to the scanning electron beam. By geometric symmetry, it is apparent that the signal of detector No. 3 is basically a time-reversed version of the signal from detector No. 1 (see Fig. 1). Detector Nos. 1 and 3 lie on a line parallel to the scan path of the electron beam; hence, we refer to these two as the on-axis detectors. Detector Nos. 2 and 4 are the off-axis detectors. This paper deals with the simulation of the on-axis detector signals. For comparison, Fig. 2 shows an actual output signal for a $5\text{-}\mu\text{m}$ -wide and $0.57\text{-}\mu\text{m}$ -deep groove in bare silicon obtained from the IBM EL-2 at Rensselaer Polytechnic Institute. This signal is from detector No. 1.

The conventional approach to the modeling of the backscattered electrons employs the Bethe continuous slowing-

down approximation (CSDA) model in a Monte Carlo simulation program.^{2,3} In the CSDA model, the mean free path of an electron is calculated after each scattering event. Sequential collisions result in electron energy loss and eventual removal from the backscattered component if the substrate surface is not reached. The Monte Carlo simulation follows the trajectories of a preselected number of electrons. To obtain proper statistical significance, a large number of electron trajectories must be simulated, resulting in considerable computation time.⁴ In the approach presented here, a simple physical model, which lends itself to rapid computation, is shown to give substantial agreement with experimental results. This is an important milestone in achieving increased

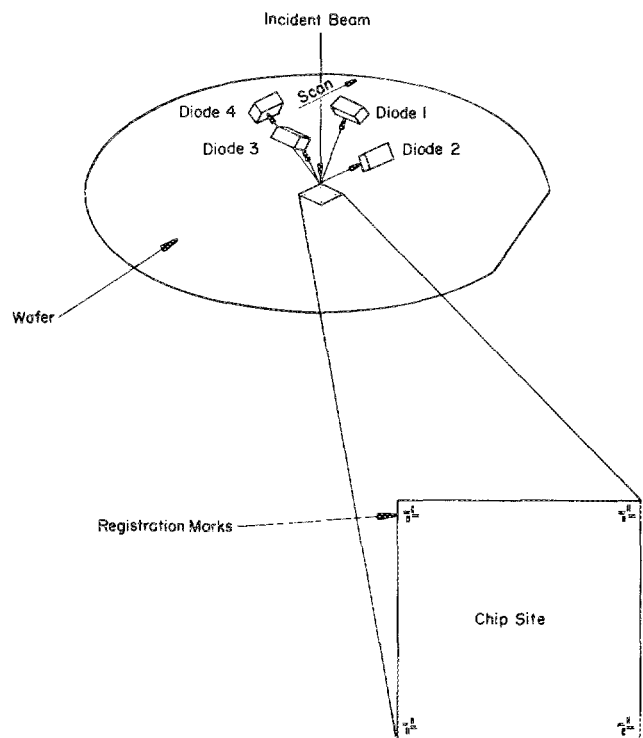


FIG. 1. E-beam pattern registration at chip site.

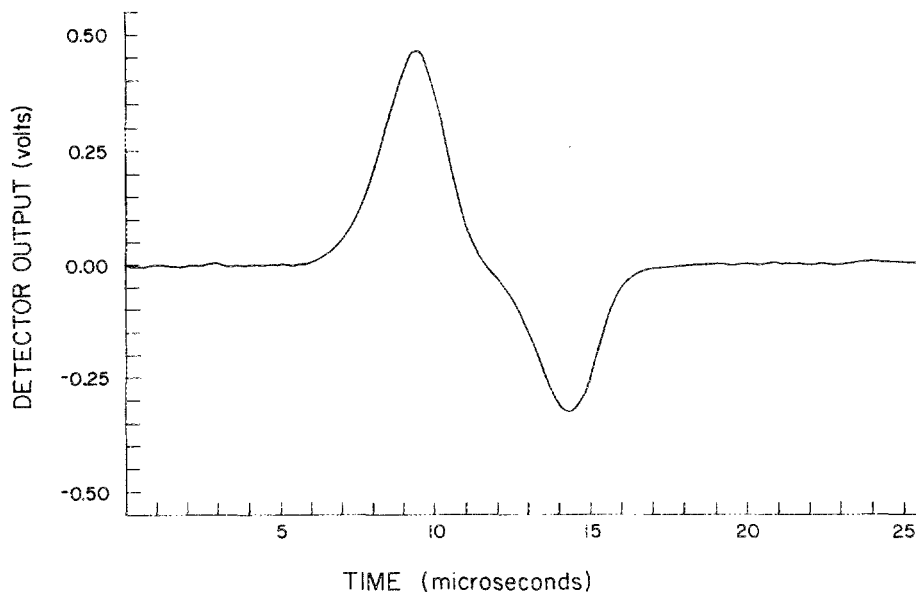


FIG. 2. Registration signal for $5 \times 0.57 \mu\text{m}$ mark.

registration speed and overlay accuracy in e-beam lithography through the use of a complete simulation and analysis program, named PEGASUS.⁵ The physical model, along with a number of improvements, is embodied in a computer program called BETTER (for backscattered electron topology transformation for enhanced registration).

There are two aspects of the overall pattern registration process which can be improved through the use of the model presented in this paper. First, the existence of a simple and accurate model reduces the need to produce wafers for experimentation. Optimization of the mark topology can be accomplished through simulation. Section III of this paper, regarding "figure of merit" shows how a simple model can aid in design of registration schemes. Secondly, the use of correlation techniques on the detector signal results in improved pattern registration performance. A robust model accurately generates the unknown signal which is needed in any correlation detector.

II. PHYSICAL BACKSCATTER MODEL

Several approaches to the modeling of the penetration of electrons in a solid have been previously reported. In one approach⁶ electrons diffuse uniformly in all directions due to multiple collisions in the solid. A second approach⁷ ignores the diffusing effect of multiple collisions and deals only with electrons elastically scattered through large angles. Archard⁸ united these two approaches and assumed that both processes occur together.

In our approach to developing an efficient registration signal model, we have used an electron "absorption" process, rather than the conventional Rutherford backscattering and CSDA mechanisms. In this context, "absorbed" electrons are removed from the backscattered beam and therefore do not reach the detector. The assumption is made that the rate of electron absorption, dn_e/dx , is proportional to the number of electrons present at a given point x in the material:

$$dn_e/dx = -\alpha n_e(x), \quad (1)$$

where α is the effective absorption coefficient. Since the detector signal S_d is proportional to the number of electrons detected, upon solving this differential equation we obtain the following relationship:

$$S_d = ke^{-\alpha x}, \quad (2)$$

where k is a constant determined empirically. From Eq. (2), it is seen that the signal displays an exponential dependence on the traversed distance through the substrate. As seen in Fig. 3, the presence of the registration mark drastically changes the path length and therefore affects the registration signal. The absorption model presented above was motivated by the observation made by Davis⁹ relating modulation of the signal by the registration mark to the path length of the backscattered electrons.

If the registration mark is fabricated in a material different from the substrate, Eq. (2) can easily be extended to include absorption in the two materials:

$$S_d = ke^{-\alpha_1 x_1 - \alpha_2 x_2}, \quad (3)$$

where x_1 and x_2 are the distances traveled through each material and α_1 and α_2 are the respective absorption coefficients.

At each position as the beam is scanned across the registration mark (see Fig. 3), the distance x which the backscattered beam travels through the materials has to be calculated. For the geometry of the EL-2 (i.e., detector size and location relative to the mark), the detector is sufficiently removed from the point of backscattering to allow the assumption of a narrow acceptance angle. For an infinitesimally narrow beam, the backscattering is modeled as occurring at a single point on the path of the incident beam, a distance D , below the surface (Fig. 3). While the backscattering occurs randomly at all angles, the component reaching the detector was taken to be defined by an infinitely narrow acceptance cone at the center of the detector. However, contributions from all components within the acceptance cone can be included by appropriately shifting the detector

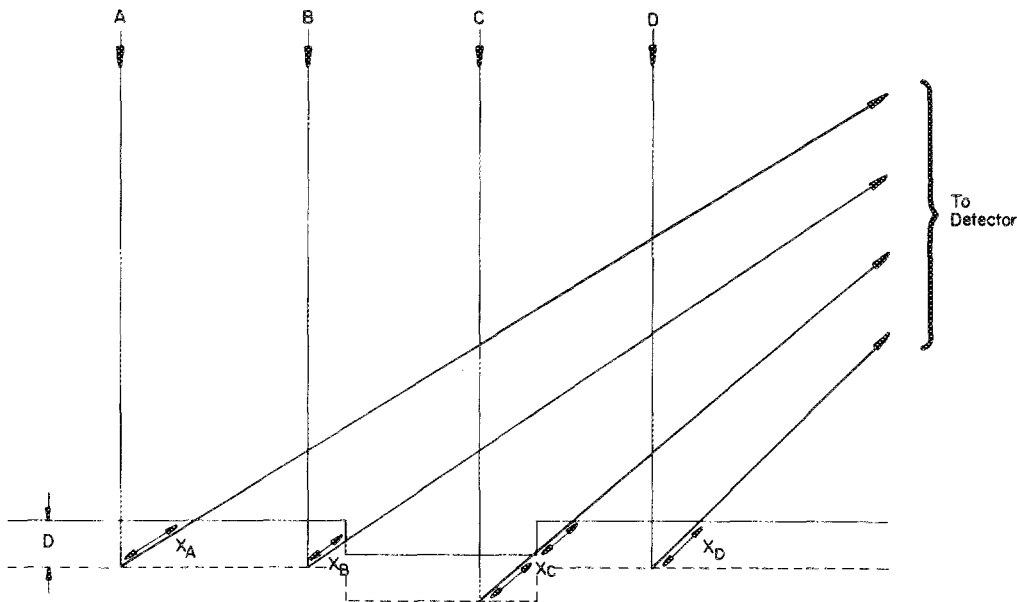


FIG. 3. Schematic for backscattering from infinitesimally narrow incident beam through silicon mark.

coordinates. The distance D is usually taken to be one half the range of electrons into the material.⁹

Generalization of the method to include a weighted spatial distribution of returns from various depth distances D is straightforward. Weights for the distribution can be surmised by examining a sufficiently large number of runs of Monte Carlo simulation to establish how many electrons on the average emerge (with sufficient energy) from the various depths. When the mark topology varies in such a way as to alter the results of the Monte Carlo simulation at different points of entry into the resist or the substrate, then a discrete number of locations can be selected for detailed simulation. Weight distributions for points along the mark topology in between those chosen for simulation can then be obtained by interpolation. The choice of the density of points chosen for simulation is somewhat subjective, but enough must be taken so that the introduction of additional detailed calculations does not lead to significant changes in the final result. This generalization is not discussed in this paper because use of the single depth model produced simulations which were accurate to within 5% for all of the examples examined and compared with experimental data.

The program SCATTER,¹⁰ which is a component of BETTER, simulates the registration signal for the case of an infinitesimally narrow beam. SCATTER calculates x for each of a finite number (typically 512) of incident beam positions and then computes the values of the detector output waveform using Eq. (2). The program takes as input a data set containing specifications of mark and resist topology, resist density, detector position, beamwidth, absorption coefficient, and penetration depth D . Figure 4 shows an example of mark and resist topologies used in the SCATTER simulation. Note that the topology of the resist is specified independently of the topology of the mark. SCATTER is capable of simulating registration signals for any arbitrary fiducial mark as long as the mark and resist profiles are piece-wise linear.

The next sections discuss enhancements to the basic SCAT-

TER model included in the BETTER program. The major improvements are obtained by considering effects such as finite beamwidth and system band limiting.

A. Finite beamwidth

Figure 3 shows four different incident beams with their associated backscattered "reflections." Each of these beams is infinitesimally narrow in the elementary model. To simulate the detector output given by a finite-width beam, one obtains the summation of many infinitesimally narrow beams which are infinitely close together. This approach leads to the convolution of the infinitesimally narrow beam with the spatial distribution of beam current density present in a real system. This assumes that the process is linear, that is to say, that the detector output due to two or more infinitesimally narrow beams is equal to the sum of the outputs due to each of the beams. In practice, to obtain the detector output given by a finite-width beam one uses a linear filter characterized by an impulse response equal to the spatial distribution of beam current density.

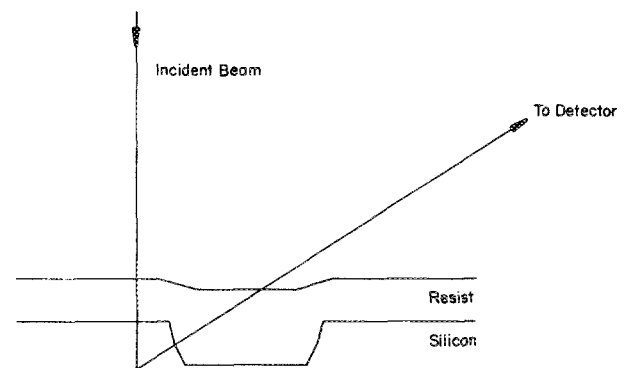


FIG. 4. Sample mark and resist topologies.

There are several ways to implement this filter.¹¹ This effect is an option in BETTER, but in general, it may be implemented as a discrete convolution (i.e., a moving average filter). A uniformly distributed beam is assumed, with user defined width. The detector output may be plotted as a function of beam position, where beam position is defined as the center of the finite-width beam.

B. Band limiting

The backscatter detectors feed the front end of the signal processing circuitry. Typically, as in the EL-2 system, there is a low-pass filter stage at that point to limit high-frequency noise. The EL-2 has a single pole filter at 0.94 MHz for this purpose.

The second enhancement in BETTER is the discrete equi-

valent of this single-pole, low-pass filter. Many references^{11,12} provide guidelines for the design of such filters.

By cascading the physical backscatter model with the finite beamwidth and band-limiting filters described above one can generate the simulations shown in Figs. 5(a) and 5(b) for marks of the same depth ($0.57\ \mu\text{m}$) and two different widths (5.0 and $2.0\ \mu\text{m}$), each covered with $1.45\ \mu\text{m}$ of polymethylmethacrylate (PMMA). The solid lines show the actual registration signals from detector No. 1 for each mark, while the dashed lines are the physically filtered SCATTER simulations. All actual registration signals shown in this paper are averaged over eight scans.

Based on the model, one can gain insight into the various features of the registration signal. For example, the inequality in the amplitudes of the positive and negative lobes is

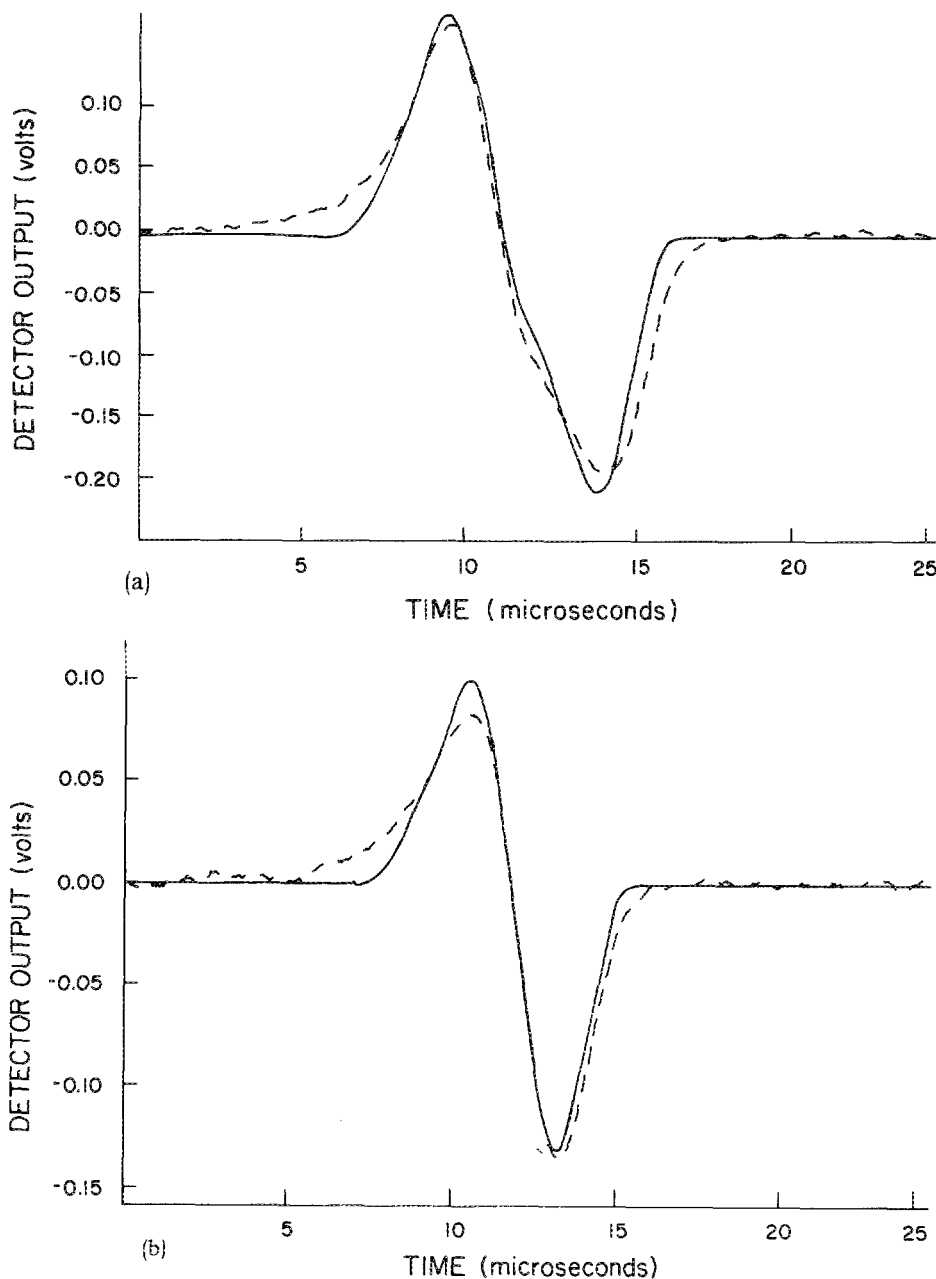


FIG. 5. Scatter simulations (dashed) vs experimental data (solid) from detector No. 1 for marks of various widths, with $1.45\ \mu\text{m}$ nominal resist thickness: (a) $5.0 \times 0.57\ \mu\text{m}$ mark and (b) $2.0 \times 0.57\ \mu\text{m}$ mark.

TABLE I. Integral-squared error criteria.

	Mark width (microns)		
	1	2	5
ISE	3.68%	2.98%	4.15%

explained by the difference in variation of the path lengths as the beam traverses the leading and trailing edges of the mark.

The sampling rate used in the simulation is high enough to properly sample the signal even if a significantly faster scan speed (and resulting higher signal frequency content) are employed.

C. Performance evaluation

To quantitatively evaluate the agreement between the physical backscatter model and actual data, a specific criterion is required. For the backscattered signal case discussed here, the error is calculated by computing the integral of the squared difference between the data and simulation curves, and then normalizing that value by the integral of the square of the data curve. The resulting value is called the integral-squared error (ISE) criterion. The ISE values shown in Table I for three topologically distinct cases are reasonable, indicating that one can accurately simulate the registration signal due to a variety of mark topologies.

III. FIGURE OF MERIT

Let us now consider an application of the registration signal model. When designing registration marks, a particular criterion must be adopted as a measure of "goodness". Equation (4) depicts a reasonable formula used to evaluate a given registration mark, termed the figure of merit (FOM). The numerator represents the energy (voltage squared) in the registration signal while the denominator is the number

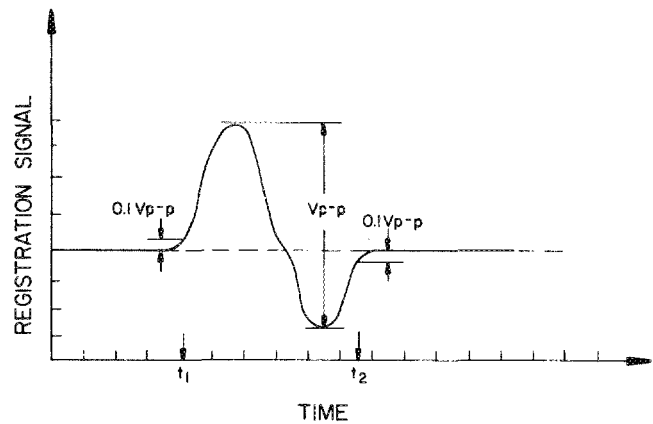


FIG. 6. Definition of FOM threshold limits.

of samples (or amount of time) between signal threshold values (see Fig. 6) of the waveform in question:

$$\text{FOM} = \frac{\sum (V_i)^2}{\text{time between threshold points } (t_2 - t_1)} \quad (4)$$

Note that the FOM has units of watts and as such is a measure of the power in the signal produced by a given mark. The threshold level for the FOM calculation is usually set at 10%–20% of the peak-to-peak value of the registration signal, as shown in Fig. 6. This level is chosen such that it is low enough to maximize the signal included in the FOM while rejecting baseline noise and transients. Optimization of the registration scheme may be achieved by maximizing the figure of merit. Furthermore, if correlators are used in the registration signal detecting structure, increased signal power improves the overall performance. In this context, the FOM defined in Eq. (4) is intuitively pleasing.

IV. FLIP-AND-SHIFT

The signals from the two on-axis detectors for a 5.0- μm -wide by 0.57- μm -deep mark, with a nominal resist thickness

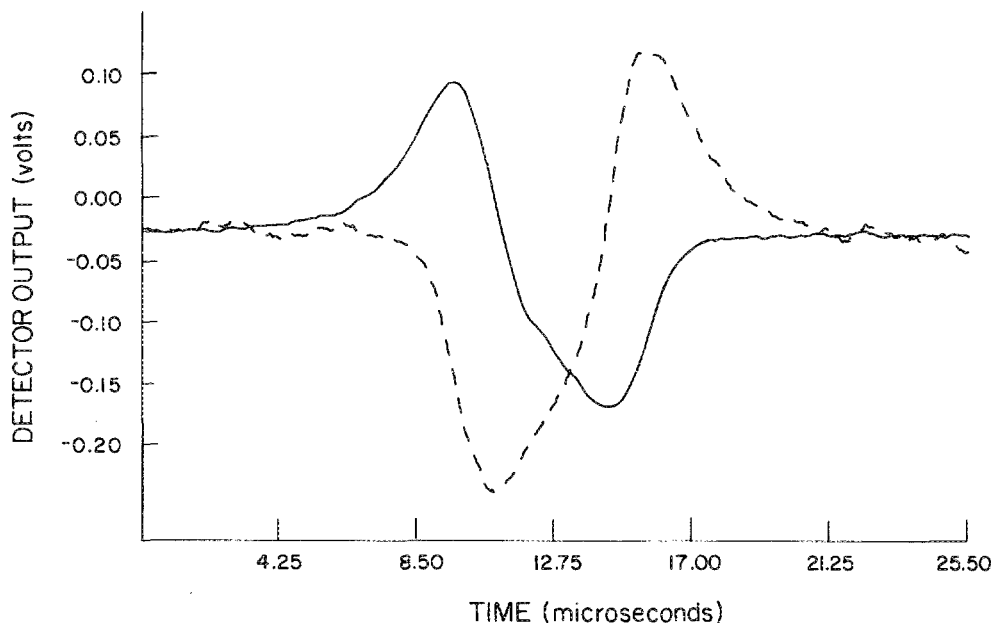


FIG. 7. On-axis signals (detector No. 1: solid; detector No. 3: dashed) from 5.0 \times 0.57 μm mark with 1.45 μm nominal resist thickness.

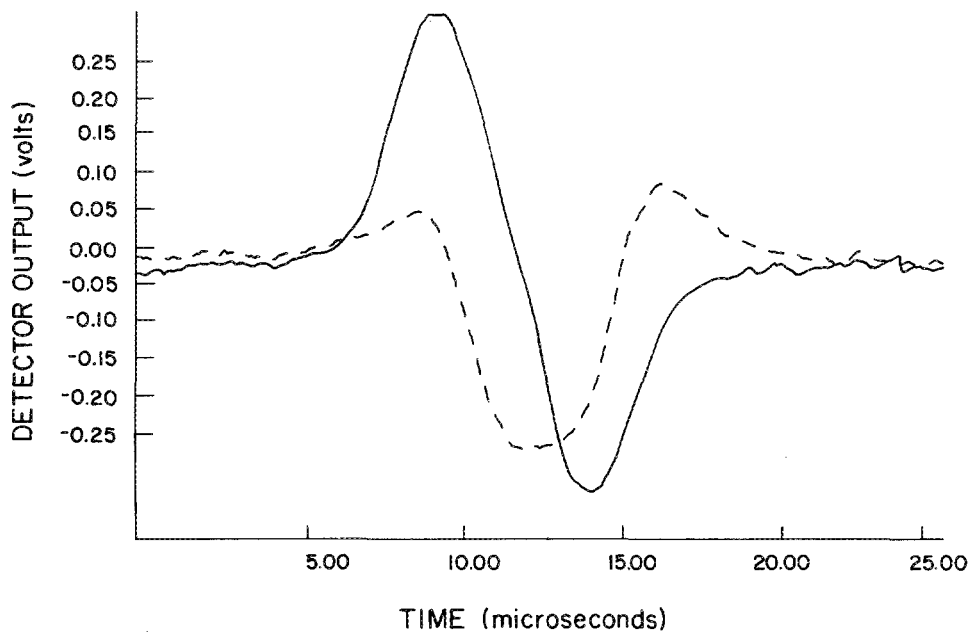


FIG. 8. Summed (dashed) and flipped-and-shifted (solid) on-axis signals from $5.0 \times 0.57 \mu\text{m}$ mark with $1.45 \mu\text{m}$ resist.

of $1.45 \mu\text{m}$, are shown in Fig. 7. To obtain optimal registration accuracy and speed, the information in these signals must be combined in an efficient way. The composite signal obtained from the addition of these individual signals is shown in the dashed line in Fig. 8, and the FOM's for each of six cases of added signals are listed in Table II(a).

Note that the two signals in Fig. 7 are close to being time-reversed versions of each other. The location of the mark in the corner of the field results in different angles between the mark and detector Nos. 1 and 3, respectively. This, in turn, results in slightly different signal attenuations for the two cases, and a small deviation from perfect time reversal. The combination of the nearly odd symmetry of each individual signal with near-symmetry in time tends to produce a cancel-

lation effect when the signals are added together. Thus, it would appear that subtraction of the signals, coupled with an appropriate time shift, would yield a composite signal with much greater power. Experimentation with the BETTER model has produced a method for implementing this.

The solid curve in Fig. 8 illustrates the composite signal produced by subtracting the signal from the first detector from the second, after the former is optimally shifted to the left. Similar signals from $2.0 \times 0.57 \mu\text{m}$ marks are shown in Fig. 9. The FOM's for each of six cases of flipped-and-shifted signals are shown in Table II(b) for both bare silicon and resist-coated marks. Note that the FOM is significantly higher in all cases of flip-and-shift, with the maximum increase being in excess of 250% for the 2.0- and $5.0\text{-}\mu\text{m}$ -wide bare silicon marks.

The amount of shift required to yield the optimum signal is constant for any given mark design, regardless of the error in wafer positioning. Thus the information needed for pattern alignment is not lost during the time shift.

Refinements of the model are currently focusing on more accurate descriptions of the topology of the cross section of the registration mark, which strongly influences the resultant signal.

Investigation is also continuing on the refinement of the absorption formula. Monte Carlo simulations of the number of backscattered electrons resulting from scanning silicon layers of various thicknesses are being used to assist in the determination of the precise coefficients needed in these formulas.

V. SUMMARY

A new approach to the modeling of e-beam pattern registration was presented. The physical model is based on absorption-like mechanism for the backscattered electrons. Good agreement between experimental data and simulation is obtained.

TABLE II. FOM (10% threshold): (a) summed signals and (b) flipped-and-shifted signals. (All values in mW.)

(a) Summed signals from opposing detectors			
	Mark width (microns)		
	2	5	10
No resist	73.5	81.7	43.0
$1.45 \mu\text{m}$ PMMA	16.6	18.2	28.7
(b) Optimally shifted and subtracted signals			
	Mark width (microns)		
	2	5	10
No resist	258.4	289.0	56.9
$1.45 \mu\text{m}$ PMMA	28.4	49.2	48.3

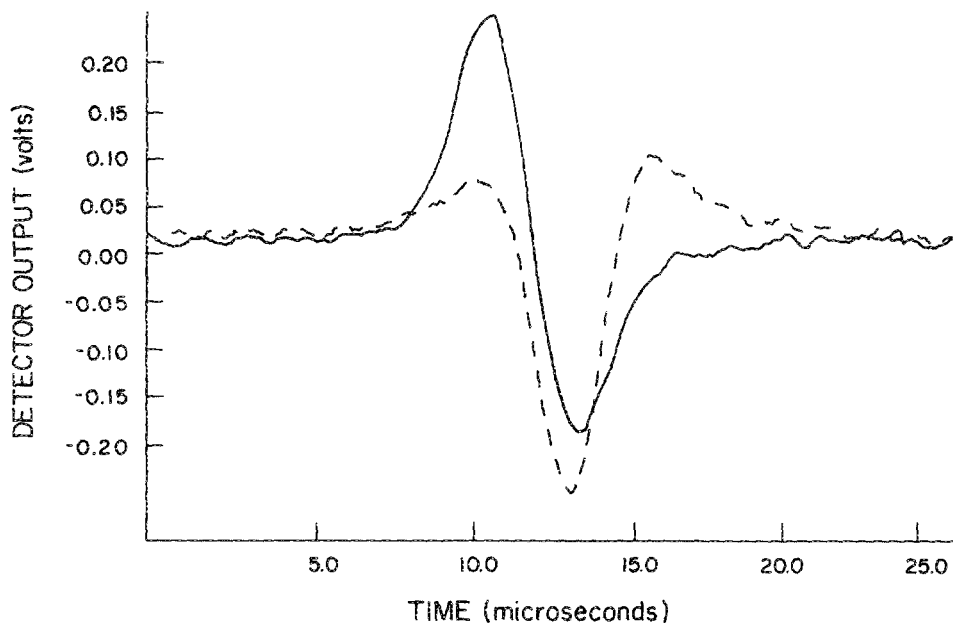


FIG. 9. Summed (dashed) and flipped-and-shifted (solid) on-axis signals from $2.0 \times 0.57 \mu\text{m}$ mark with $1.45 \mu\text{m}$ resist.

The model was used to develop a new approach, flip-and-shift, to the combination of signals from two detectors. A figure of merit (FOM) was defined, and FOM values for flipped-and-shifted composite signals were shown to be significantly greater than FOM values for summed detector signals.

ACKNOWLEDGMENT

The authors gratefully acknowledge partial support of this program by IBM Corporation.

¹E. V. Weber, in *Fine Line Lithography*, edited by R. Newman (North-Holland, Amsterdam, 1980), Chap. 5.

²I. Adesida, T. E. Everhart, and R. Shimizu, *J. Vac. Sci. Technol.* **16**, 1743 (1979).

³Y. C. Lin and I. Adesida, *Appl. Phys. Lett.* **36**, 672 (1980).

⁴K. Murata, *J. Appl. Phys.* **45**, 4110 (1974).

⁵J. L. Morgenstern, M. S. thesis, Rensselaer Polytechnic Institute, 1984.

⁶H. A. Bethe, *Ann. Physik* **5**, 325 (1940).

⁷T. E. Everhart, *J. Appl. Phys.* **31**, 1483 (1960).

⁸G. D. Archard, *J. Appl. Phys.* **32**, 1505 (1961).

⁹D. E. Davis, *IBM J. Res. Dev.* **24**, 545 (1980).

¹⁰J. L. Morgenstern, A. J. Steckl, D. C. King, M. A. Bourgeois, and G. R. Redinbo, *J. Electrochem. Soc.* **83-2**, 329 (1983).

¹¹G. F. Franklin and J. D. Powell, *Digital Control of Dynamic Systems* (Addison-Wesley, Reading, PA, 1980).

¹²A. V. Oppenheim and R. W. Schaffer, *Digital Signal Processing* (Prentice-Hall, Englewood Cliffs, NJ, 1975).